

# Low Field (10 mT) Pulsed Dynamic Nuclear Polarization

Marcello Alecci<sup>1</sup> and David J. Lurie

*Department of Bio-Medical Physics and Bio-Engineering, University of Aberdeen, Foresterhill, AB25 2ZD, Aberdeen, UK*

Received May 28, 1998; revised January 26, 1999

**EPR irradiation by a train of inverting pulses has potential advantages over continuous-wave EPR irradiation in DNP applications; however, it has previously been used only at high field (5 T). This paper presents the design and testing of an apparatus for performing pulsed DNP experiments at 10 mT with large samples (17 ml). Experimental results using pulsed DNP with an aqueous solution of a narrow-linewidth paramagnetic probe are presented. A maximum DNP enhancement of about  $-36$  with a train of inverting pulses (width 500 ns, repetition time 4  $\mu$ s) was measured. A preliminary comparison showed that, when the same enhancement value is considered, the pulsed DNP technique requires an average power that is about three times higher than that required with the CW irradiation. However, for *in vivo* DNP applications it is very important to minimize the average power deposited in the sample. From the experimental results reported in this work, when considering the maximum enhancement, the pulsed technique requires only 2% of the average power necessary with the CW DNP technique. We believe that this reduction in the average power can be important for future DNP studies with large biological samples.** © 1999 Academic Press

**Key Words:** DNP; EPR; pulsed; CW; single electron contrast agents.

Dynamic nuclear polarization (DNP) is a double-resonance technique that permits the enhancement of the polarization of nuclei in samples containing paramagnetic species (1). DNP has many applications in physics, chemistry and biology. For example DNP associated with Magnetic Resonance Imaging (MRI) techniques permits the detection of stable nitroxide free radicals in large animals (this technique is known as proton electron double resonance imaging (PEDRI)) (2–4). Nitroxides have been widely used as probes of biophysical and biochemical properties such as (5) electrical potential, pH, temperature, oxygen concentration, molecular mobility of proteins and lipids in membranes, and enzyme activity. Nitroxides have also

been studied as potential contrast agents for MRI (6). More recently, nitroxides have been used as tracers for low frequency electron paramagnetic resonance (EPR) imaging (7) and in DNP cross-polarization experiments with biomolecules in frozen solutions (8).

Double-resonance experiments involving two-spin systems can be performed with either continuous wave (CW) or pulsed excitation of the transitions of one spin while observing the other spin. After the theoretical prediction of Overhauser in 1953 (9), the first double-resonance experiment using the CW technique was performed by Carver and Slichter (10). The double-resonance pulsed technique was originally demonstrated by Solomon (11) for two nuclear species, this method being known as the transient nuclear Overhauser effect. In Solomon's experiment the relaxation times of the two nuclear species (<sup>1</sup>H and <sup>19</sup>F) were of the same order ( $\sim 1$  s). For each acquisition cycle only one inverting pulse ( $\pi$  pulse) was applied at the resonant frequency of the proton spins; the longitudinal magnetization of the fluorine was detected and showed a transient decay in a time comparable to the longitudinal relaxation times.

The majority of DNP experiments have been performed with CW irradiation of the EPR transitions. Recently, pulsed DNP has been proposed by Un and co-workers (12) for spectroscopic studies at very high field (5 T). Their main goal was the detection of <sup>13</sup>C spectra (from a powder sample of an organic conductor) with increased signal-to-noise ratio and decreased average microwave power deposited in the sample (12). The pulsed DNP technique was demonstrated indirectly by dividing the experiment into two phases: (i) excitation of the electron spins with a train of microwave (140 GHz) pulses, enhancing the proton polarization in a time comparable with the nuclear relaxation times; (ii) transfer of the proton polarization to the <sup>13</sup>C spins via a conventional cross-polarization method. Un and co-workers stated that, for a given average EPR power and with an inhomogeneously broadened EPR spectrum, a model calculation predicts higher pulsed DNP enhancement with respect to CW DNP (12).

In this Communication we describe the design and testing of a pulsed DNP ( $\pi$ DNP) apparatus operating at very low field (10 mT) suitable for detection of free radicals in large aqueous

<sup>1</sup> On leave from IPSIA and Istituto Nazionale Fisica Materia, Dipartimento di Scienze e Tecnologie Biomediche, Universita' dell'Aquila, Via Vetoio, 67100, L'Aquila, Italy. Address correspondence to Dr. M. Alecci, FMRI Centre, Department of Clinical Neurology, University of Oxford, John Radcliffe Hospital, Headington, Oxford, OX3 9DU, England; E-mail: alecci@fmrib.ox.ac.uk.

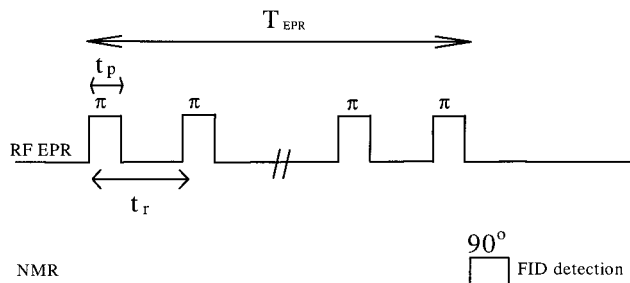


FIG. 1. Diagram of the sequence used for pulsed DNP.

samples. Direct experimental evidence of the  $\pi$ DNP technique is shown with a water-soluble single line triarylmethyl paramagnetic label. The main goal of this  $\pi$ DNP technique at low field is to increase the signal-to-noise ratio and/or to decrease the average RF power deposited in the sample.

The sequence for  $\pi$ DNP is shown in Fig. 1, where an “ideal” train of EPR  $\pi$  pulses is considered. This means that (i) the duration of the train of  $\pi$  pulses,  $T_{EPR}$ , is longer than the longitudinal proton relaxation time  $T_{1p}$  (infinite train); (ii) the width of each  $\pi$  pulse,  $t_p$ , is very small in comparison to the electron longitudinal and transversal relaxation times  $T_{1e}$  and  $T_{2e}$  (instantaneous inversion); (iii) the pulse rise time and fall time are very short with respect to  $t_p$ ; and (iv) the bandwidth of the  $\pi$  pulse is large enough to cover the full EPR spectrum of the paramagnetic probe. Moreover, we assume that the EPR resonator dead time,  $T_D$ , is smaller than the pulse repetition time,  $t_r$ . These conditions influence the design of the hardware and the operating conditions of the  $\pi$ DNP instrument as discussed in the following.

The  $T_{1e}$  and  $T_{2e}$  of the paramagnetic sample are important for the definition and optimization of the  $\pi$ DNP experimental requirements. As explained in the following, to reduce the hardware constraints paramagnetic samples with  $T_{1e} \approx T_{2e} \geq 1 \mu\text{s}$  are required. Alternatively, because  $T_{2e}$  is inversely proportional to the linewidth of the paramagnetic sample, very narrow lines are required ( $\sim 5 \mu\text{T}$ ). Nitroxide free radicals have been used extensively in previous *in vivo* EPR/DNP studies (2–8, 13, 14). Unfortunately, they have large linewidths ( $\sim 150 \mu\text{T}$ ) and the measured relaxation times are too short ( $\sim 350 \text{ ns}$ ) (15, 16). Perdeuterated nitroxides present much narrower EPR lines ( $\sim 20 \mu\text{T}$ ) and the linewidth is highly sensitivity to oxygen concentration, making these compounds very interesting for biological applications (13).

Recently, a novel class of water-soluble triarylmethyl (TAM) compounds have been proposed for *in vivo* EPR and DNP studies (17). The structure, synthesis, and characterization of the TAM agents have been reported elsewhere (18). The TAM free electron contrast agents have one major very narrow EPR line and a number of small satellite EPR lines. These satellite lines arise from the hyperfine coupling of the free

electron with the  $^{13}\text{C}$  nuclei of the contrast agent. A detailed description of the EPR and DNP spectral properties of TAM compounds similar to that used in the present work has been recently reported (19, 20). Kuppusamy and co-workers showed that from CW EPR studies at 1.2 GHz the linewidth of an analogue of TAM is  $\sim 6 \mu\text{T}$  in absence of oxygen (21). From CW DNP measurements at about 10 mT, Konijnenburg and co-workers found that another analogue of TAM in water solution has  $T_1 \times T_2 \cong 2.9 \times 10^{-12} \text{ s}^2$  (22). The properties of the TAM compounds are appropriate to test the  $\pi$ DNP technique. A small amount was obtained as a gift from Nycomed Innovation AB (Malmö, Sweden) and was used for preliminary  $\pi$ DNP studies at 10 mT. A 1 mM water solution of TAM contained in a 17 ml sample tube (diameter 23 mm) was used. The solution was deoxygenated with a flux of nitrogen for about 2 h to reduce line broadening due to paramagnetic relaxation.

Figure 2 shows a block diagram of the RF hardware designed and tested in this work for  $\pi$ DNP at 10 mT. A pulse generator (Lyon Instruments, model PG71) was used to generate a TTL gating signal with variable width of 100 to 500 ns and period of 1 to 20  $\mu\text{s}$ . The TTL signal was applied to the external gate input of an RF source (Gigatronics, model 610) that provided the EPR frequency of about 280 MHz with a maximum nominal output of +17 dBm. The external gating of the RF source could be disabled, allowing CW DNP measurements. A low-power directional coupler (Mini Circuit, ZAD-10-1) was inserted between the RF source and the power amplifier (Kalmus, 400 FC), and its coupling output CPL ( $-10 \text{ dB}$ ) was connected to a high-frequency oscilloscope (Philips, PM 3295A) for monitoring of the low-power transmitted (TX) pulses. The power amplifier is a class-A linear amplifier that covers a frequency range of 1.5 to 400 MHz. When operated in CW mode the maximum nominal power is 60 W (gain 48 dB). A homebuilt, high-power directional coupler (23) was used for

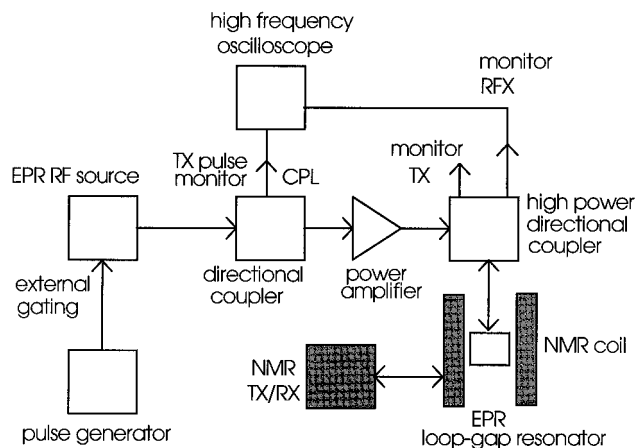


FIG. 2. Schematic diagram of the radiofrequency hardware developed for pulsed DNP at 10 mT.

power calibration and monitoring of the TX and reflected (RFX) high-power RF pulses. The measured rise and fall times of the pulses at the power amplifier output were less than 10 ns. The measured power (incident into the EPR resonator at critical coupling) was about 13 W with nominal RF source power level of 0 dBm. An inductive loop (32 mm in diameter) positioned in a sliding mechanism was used to match the impedance of the EPR resonator to that of the RF power amplifier. All the connections for the RF signals were made with 50  $\Omega$  coaxial cable (RG 58). The NMR hardware for the detection of the water proton signal at 10 mT has been described previously (24) and is only schematically shown in Fig. 2. The NMR TX/RX originally designed for operation at 40 mT (1.7 MHz NMR frequency) was modified for operation at 10 mT by the inclusion of down- and up-frequency converters. A 70-turn solenoidal transmit/receive coil tuned to 425 kHz (dia 7.5 cm, length 7 cm) was used (23) and was placed inside a cylindrical 40  $\mu$ m copper foil shield (dia 20 cm, length 30 cm). The EPR resonator was inserted centrally within the NMR coil. Because the field of the NMR coil is coaxial with that of the EPR resonator, a variable decoupling capacitor (3–20 pF) was connected in series with the coupling loop to avoid interference on the proton free induction decay (FID).

Previous studies have shown that, for a given EPR power, the loop gap resonator gives the maximum  $B_{1e}$  field when compared to other resonator designs (25). This feature is particularly important for  $\pi$ DNP because the EPR power can be minimized. In this work a bridged one-loop one-gap resonator (LGR) was used (25). The LGR prototype was built on a Perspex cylinder (internal diameter 31 mm, external diameter 38 mm, length 30 mm). A sheet of adhesive copper tape (thickness 10  $\mu$ m) was laid on the cylinder. A PTFE sheet (thickness 10  $\mu$ m) was used as dielectric and the gap width and separation were 19 and 0.5 mm, respectively. A high-quality-factor variable capacitor ( $\sim$ 30 pF, Oxley, UK) was used to tune the LGR to the required frequency. A network analyser (Anritsu, MS3606B) and a directional coupler (Mini Circuit, ZAD-10-1) in a reflection configuration were used to measure the LGR resonant frequency ( $f_0 \cong$  280 MHz), the matching (better than 25 dB), and the loaded quality factor ( $Q_L \cong$  173 when empty).

The flip angle  $\alpha$  of the electron magnetization is given by the Breit equation (26)

$$\alpha = \gamma_e \cdot B_{1e} \cdot t_p \quad [1]$$

where  $\gamma_e = 1.79 \times 10^{11}$  rad s<sup>-1</sup> T<sup>-1</sup>,  $B_{1e}$  (T) is the RF magnetic field in the rotating frame, and  $t_p$  (s) is the width of the pulse. For a  $\pi$  pulse with  $t_p = 200$  ns, a peak  $B_{1e}$  amplitude of about 90  $\mu$ T is required. The magnitude of the LGR efficiency parameter,  $\Lambda$ , determines the power required for the  $\pi$  pulse. It has been shown that for the LGR (25)

$$\Lambda = \frac{B_{1e}}{\sqrt{P}} \propto \sqrt{\frac{Q_L}{f_0 \cdot r_0^2 \cdot Z}}, \quad [2]$$

where  $P$  is the power incident on the resonator,  $Q_L$  is the loaded quality factor, and  $r_0$  and  $Z$  are the radius and the length of the LGR, respectively. The method of the perturbing metallic sphere (27) was used to measure  $\Lambda$  and we found that for the empty LGR  $\Lambda \cong 37 \mu$ W<sup>1/2</sup>. The insertion of 11 ml of physiological saline solution reduced the quality factor ( $Q_L = 86$ ) and the measured  $\Lambda$  was about 20  $\mu$ W<sup>1/2</sup>. By using these measured values, the required peak power incident in the resonator is about 1 W with the empty LGR and 3 W with the physiological saline solution. The power amplifier provides a maximum power of only 60 W, and for this reason we were restricted to using pulses with widths of 500 ns. Several factors influence the accuracy with which the  $B_{1e}$  amplitude can be measured: RF source power output level; gain and bandwidth of the RF power amplifier; coupling coefficient and bandwidth of the high-power directional coupler; oscilloscope vertical calibration; and matching and efficiency factor of the EPR resonator. We estimated that  $B_{1e}$  was measured with an accuracy of about  $\pm 20\%$ . Consequently, it was necessary to regulate experimentally the peak EPR power (or the pulse width) around the expected value to select the inverting pulses.

Another factor to take into account with  $\pi$ DNP at low field is the LGR ringing time. The applied  $\pi$  pulse produces a buildup and decay of  $B_{1e}$  in the LGR with time constant  $\tau$  given by (26)

$$\tau = \frac{Q_L}{2\pi \cdot f_0}, \quad [3]$$

where  $f_0$  is the frequency of operation. The dependence of  $\tau$  on the inverse of the frequency penalizes low-field  $\pi$ DNP applications. For example, at 280 MHz and assuming a quality factor of 1000, we have that  $\tau \cong 570$  ns. The  $\tau$  value for our LGR was measured using a power reflection method (26): the high-power directional coupler and high-frequency oscilloscope (see Fig. 2) were used to monitor the buildup and decay of the reflected (RFX) power. It was found that  $\tau \cong 160$  ns for the empty LGR and  $\tau \cong 110$  ns with 23 ml of deionized water ( $Q_L = 155$ ). If we assume that for  $\pi$ DNP experiments the resonator dead time is  $T_D \approx 5 \cdot \tau$ , this means that with aqueous samples the repetition time should be chosen to be longer than 1  $\mu$ s. However, it is important to note that this requirement is strongly dependent on the nature of the free radical under study and the loading effect of the sample on the LGR.

$\pi$ DNP experiments were carried out using 1 mM deoxygenated TAM in aqueous solution (17 ml). FIDs were acquired without EPR irradiation (see Fig. 3a) to obtain the reference signal for the calculation of the DNP enhancement. FIDs were also acquired following a train of  $\pi$  pulses under the following

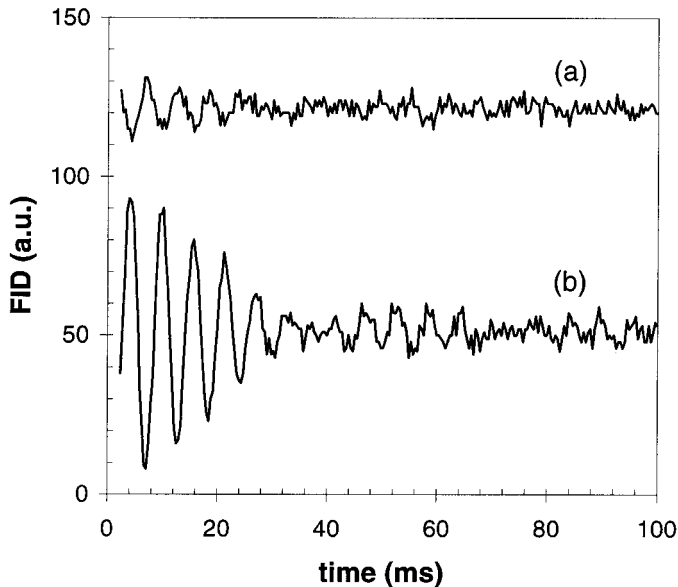


**FIG. 3.** Proton FID detected: (a) without EPR irradiation; and (b) with a train of EPR inverting pulses [EPR irradiation frequency 279.65 MHz; EPR power  $-8$  dBm at the RF source (peak power of 2 W in the resonator);  $t_p = 500$  ns;  $t_r = 12$   $\mu$ s;  $T_{\text{EPR}} > 500$ ms]. The paramagnetic sample was 1 mM of TAM in deionized water.

experimental conditions: EPR irradiation frequency 279.65 MHz; EPR power of  $-8$  dBm at the RF source;  $t_p = 500$  ns;  $t_r = 20$   $\mu$ s;  $T_{\text{EPR}} \geq 500$  ms. The  $\pi$ DNP enhancement was calculated as (*I*)

$$A = \frac{I_z - I_0}{I_0}, \quad [4]$$

where  $I_0$  and  $I_z$  are the peak-to-peak amplitudes of the FID without and with the EPR irradiation, respectively. As reported in Fig. 3b, the FID showed a significant increase of the amplitude and the  $\pi$ DNP enhancement was about  $-6$  (the minus sign is due to the phase inversion of the FID with respect to the reference signal). This EPR power of  $-8$  dBm corresponds to a peak power of about 2 W in the resonator. The duty cycle of the train of pulses was 3%, and this gives an average peak power of about 60 mW at the sample.

The theory of pulsed DNP (*12*) predicts that the application of EPR pulses of arbitrary amplitude that produces a deviation of the longitudinal electron magnetization from the equilibrium value will enhance the proton FID signal. However, only the “exact” EPR power level corresponding to the  $\pi$  pulse will produce the maximum deviation of the longitudinal electron magnetization from the equilibrium value (i.e., maximum DNP enhancement). Any further increase of the power level will reduce the FID enhancement, and a power level corresponding to a flip angle of  $2\pi$  should give zero enhancement. As pointed out in the experimental section, several factors influence the

accuracy with which the RF magnetic field can be measured. Because of the modest accuracy ( $\pm 20\%$ ) of the measured RF power, for a given EPR pulse width the peak EPR power should be experimentally regulated around the expected value corresponding to the inverting pulse. For these reasons,  $\pi$ DNP experiments were performed with a wide range of EPR power (between  $-40$  dBm and  $+16$  dBm at the RF source) using repetition times of 12 and 4  $\mu$ s. The pulse width was maintained at a constant value of 500 ns. It was found that the FID amplitude was sensitive to the power level of the irradiating EPR pulses. The FID peak-to-peak amplitude was used to calculate the  $\pi$ DNP enhancement according to Eq. [4]. We believe that the total number of pulses is important to establish how the enhancement converges to the maximum achievable value. Unfortunately, with the present experimental apparatus we are unable to clarify this particular aspect. For this reason we used a train of EPR pulses with a total duration that is much longer than the longitudinal proton relaxation time ( $T_{\text{EPR}} \geq 500$  ms).

The experimental results reported in Fig. 4a for a repetition time of 12  $\mu$ s show that (i) the  $\pi$ DNP enhancement follows a steady increase from zero to about  $-8$  for EPR power levels up to  $-12$  dBm, and (ii) for higher power, the enhancement shows an oscillating behavior, with a first maximum of  $-11$  obtained at power of  $-8$  dBm and a second maximum of  $-10$  at power of  $+7$  dBm. The saturation limit of the power amplifier meant that it was not possible to extend the measurements to higher power levels. The results obtained with a shorter repetition time of 4  $\mu$ s (Fig. 4b) show a similar oscillating behavior, with

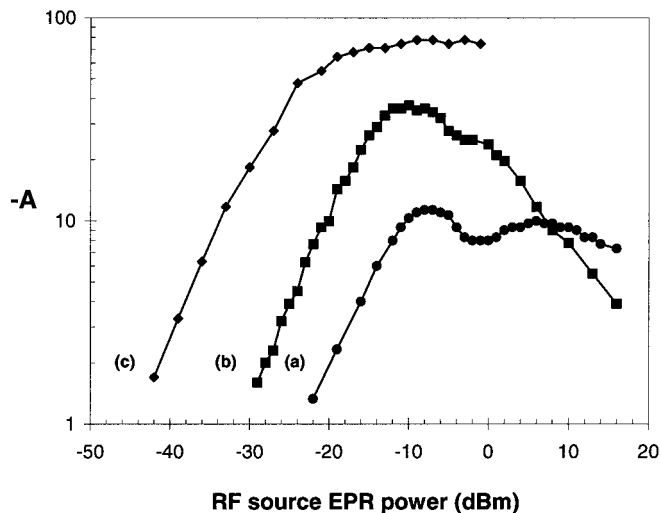


**FIG. 4.** DNP enhancement versus the peak EPR irradiating power obtained with (a) a train of pulses with  $t_r = 12$   $\mu$ s; (b) a train of pulses with  $t_r = 4$   $\mu$ s; and (c) CW irradiation. The EPR power of 0 dBm at the RF source corresponds to 13 W of peak power incident on the loop gap resonator. The paramagnetic sample was 1 mM of TAM in deionized water, and the EPR acquisition parameters were: EPR irradiation frequency 279.65 MHz;  $T_{\text{EPR}} \geq 500$  ms;  $t_p = 500$  ns.

a first maximum  $\pi$ DNP enhancement value of  $-36$  obtained at a power of  $-10$  dBm. A second maximum in the  $\pi$ DNP enhancement equal to about  $-25$  was observed at a power of  $-4$  dBm, although it was not as well resolved as for the longer repetition time.

These experimental results demonstrated that  $\pi$ DNP was actually being used and not merely discontinuous EPR irradiation. The observation of these two maxima in the  $\pi$ DNP enhancement is in accordance with a periodical variation of the electron spin FID amplitude as observed *directly* with a 9 GHz pulsed EPR spectrometer using nickel impurities in synthetic diamond (28). As shown in Fig. 4, the first maximum in the DNP enhancement occurs with peak power of about 1.3 W ( $-10$  dBm at the RF source) and pulse width of 500 ns. For the TAM water sample the measured efficiency factor was about  $34 \mu\text{T/W}^{1/2}$  and the corresponding flip angle is about  $174^\circ$ . As previously anticipated, the experimental errors affecting the LGR efficiency factor, the pulse width, and the peak EPR power could explain the deviation of the estimated flip angle from the theoretical value of  $180^\circ$  (inverting EPR pulse). We must point out that the minimum in the oscillating pulsed DNP enhancement curves of Figs. 4a and 4b does not reach the zero value as might be expected. This is probably due to off-resonance effects of the irradiating EPR pulse and/or inhomogeneity of the RF  $B_{1c}$  field within the sample volume. Moreover, from Figs. 4a and 4b we observe that for the shorter repetition time the oscillations in the DNP enhancement are less distinct and shifted by a few decibels with respect to the data obtained with the longer repetition time. With the shorter repetition time we are approaching the resonator dead time, and this could explain these findings.

A preliminary comparison of the enhancement obtained with the  $\pi$ DNP and the CW DNP techniques was obtained with the present apparatus. The FIDs using CW irradiation ( $T_{\text{EPR}} \geq 500$  ms) were acquired with EPR power between  $-42$  dBm and  $-1$  dBm at the RF source. The measured CW DNP enhancement reported in Fig. 4c shows a steady increase from  $-1$  to about  $-50$  for peak EPR power levels up to  $-25$  dBm. For higher power the enhancement reaches a "plateau" with a maximum value of about  $-78$  with a peak level of  $-1$  dBm. This variation of the DNP enhancement is a standard feature for CW EPR irradiation and can be explained by the progressive saturation of the EPR transition ( $I$ ). For the TAM agents Ardenkjaer-Larsen *et al.* (19) reported a CW DNP enhancement at infinite concentration of the agent and at infinite EPR irradiating power,  $A_\infty$ , of about  $-270$ . A smaller value ( $A_\infty = -233$ ) has been reported by Konijnenburg *et al.* (22) using TAM in water solutions. In our experimental conditions, we estimate that the CW saturation factor was about 0.98 and the leakage factor was about 0.33 (from the TAM relaxivity data reported in Ref. 19). This should explain why we have measured a lower CW DNP enhancement ( $A = A_\infty \cdot f \cdot s$ ) value than have other groups. Recently, a maximum enhancement of  $-60$  in the

vascular area and a value of  $-100$  in the urine bladder of living rats have been reported by Golman and co-workers (20).

It is interesting to compare the average power required by the two DNP techniques when the *same* enhancement is considered. This can be obtained from the results reported in Figs. 4b and 4c with the peak power in the range of  $-30$  to  $-10$  dBm. We observe that in this range the pulsed technique requires about 14 dBm peak power more than the CW DNP technique. This means that, when the *same* enhancement value is considered, the pulsed DNP technique requires an average power that is about three times higher than that required with the CW irradiation. Of course this comparison can be made only for enhancement values less than  $-36$ , since this corresponds to the maximum value observed with the train of pulses with 4  $\mu\text{s}$  repetition time.

For *in vivo* DNP applications it is very important to minimize the average power deposited in the sample. The results reported in Fig. 4b shows that with a train of  $\pi$  pulses (width 500 ns, repetition time 4  $\mu\text{s}$ ) the maximum DNP enhancement of about  $-36$  was obtained with a peak level of  $-10$  dBm at the RF source. From the results reported in Fig. 4c, the maximum CW DNP enhancement of about  $-78$  was obtained with a peak level of  $-1$  dBm at the RF source. In the present experimental conditions and considering the maximum enhancement achievable, the pulsed technique requires only 2% of the average power necessary with the CW DNP technique. We believe that this reduction in the average power can be important for future DNP studies with large biological samples.

Ardenkjaer-Larsen *et al.* (19) have reported  $T_{1c} = 11 \mu\text{s}$  and  $T_{2c} = 9 \mu\text{s}$  for the TAM agents in deoxygenated isotonic saline and at infinite dilution. In practical conditions, much shorter relaxation times are obtained. From DNP studies at 8.5 mT, Konijnenburg *et al.* (22) have previously reported that for 1 mM TAM in water  $T_{1c} \times T_{2c} = 2.9 \times 10^{-12} \text{ s}^2$ . Assuming a correlation time of the order of 10 ps (similar to that of small nitroxides) and considering an irradiating frequency of 280 MHz, it can be shown (15) that  $T_{1c} \approx T_{2c}$ . Thus, from the data reported by Konijnenburg *et al.* (22), we estimate that for the 1 mM TAM solution  $T_{1c}$  should be about 1.7  $\mu\text{s}$ . In the present study, the full width at half-amplitude,  $\Delta B_{1/2}$ , of TAM was derived from the CW DNP enhancement as a function of the EPR irradiating frequency (main field 10 mT). We found that for our sample  $\Delta B_{1/2} \cong 20 \mu\text{T}$ , and this gives an estimated  $T_2^*$  value of 0.5  $\mu\text{s}$ . With these values in mind, it is not surprising that the train of EPR pulses with 4  $\mu\text{s}$  repetition time is effective in increasing the maximum enhancement as compared to the pulses with 12  $\mu\text{s}$  repetition time. As the repetition time is further decreased we do not expect a decrease of the maximum enhancement. For very short repetition times the pulsed DNP technique should "converge" to the CW technique. Consequently, the oscillations in the enhancement should disappear and the enhancement should show a steady

increase as a function of power until the plateau is reached. This is approximately the behavior of the DNP enhancement reported in Fig. 4. However, we were not able to observe this transition in more detail because of the limitation due to the dead time of the EPR resonator.

In conclusion, an apparatus for  $\pi$ DNP at 10 mT has been designed and the most important experimental problems (peak EPR power, pulse width and repetition time, resonator dead time) have been addressed. The enhanced FID of protons after a train of inverting EPR pulses has been detected by using a water soluble TAM single-electron contrast agent with a very narrow ( $\sim 20$   $\mu$ T) EPR line. A maximum DNP enhancement of about  $-36$  with a train of inverting pulses (width 500 ns; repetition time 4  $\mu$ s) was measured. A preliminary comparison showed that, when the same enhancement value is considered, the pulsed DNP technique requires an average power that is about three times higher than that required with the CW irradiation. However, for *in vivo* DNP applications it is very important to minimize the average power deposited in the sample. From the experimental results reported in this work, when considering the maximum enhancement, the pulsed technique requires only 2% of the average power necessary with the CW DNP technique. We believe that this reduction in the average power can be important for future DNP studies with large biological samples. With CW DNP the saturation of an EPR line is not a linear function of the power. In particular, with large lossy samples, to achieve a high degree of saturation the corresponding EPR power can be very large or prohibitive (because of instrumental and/or SAR limitations). Of course, the use of narrow-linewidth paramagnetic agents makes it easier to achieve a given degree of CW EPR saturation. The pulsed DNP method proposed in this work aims to overcome the EPR power irradiation problem, and it is not limited to narrow-linewidth agents. We have chosen the TAM probe because the instrumental constraints are less severe and also because there is a strong interest in the use of TAM for DNP/EPR *in vivo* oximetry (17–22). Experimental evidence of the pulsed DNP technique with a perdeuterated nitroxide free radical (linewidth 87  $\mu$ T) has been reported elsewhere (31). With the present apparatus, because of the dead time of the LGR, the EPR pulse repetition time must be longer than 1  $\mu$ s. At moment this is one of the main instrumental constraints for  $\pi$ DNP at low frequency. However, in the context of pulsed EPR, several methods have been recently proposed (29, 30) to decrease the resonator dead time and are being investigated.

Finally, in this work the main experimental problems for low-field (10 mT) pulsed DNP have been addressed. However, there are many theoretical and experimental issues that need further investigation. For example, it will be very important to have a detailed theoretical comparison between the enhancement achievable with the two DNP techniques. Moreover, it will be interesting to know the dependence of the pulsed DNP enhancement on the EPR irradiation power, the EPR pulse

width and shape, EPR pulse repetition time, and the total number of pulses. We have done some preliminary work (31) and we are aware that other groups are working on this problem (J. H. Ardenkjaer-Larsen, personal communication, 1998). We hope such detailed analysis will be available in the future.

## ACKNOWLEDGMENTS

We thank Dr. J. M. S. Hutchison and Dr. J. H. Ardenkjaer-Larsen for many helpful discussions. We are also grateful to Nycomed Innovation AB for the kind donation of the TAM single-electron contrast agent. M. Alecci acknowledges the support of the European Union for a fellowship under the "Training and Mobility of Researchers" program.

## REFERENCES

1. K. H. Hausser and D. Stehlik, *Adv. Magn. Reson.* **3**, 79 (1968).
2. D. J. Lurie, D. M. Bussell, L. H. Bell, and J. R. Mallard, *J. Magn. Reson.* **76**, 366 (1988).
3. D. Grucker, *Mag. Reson. Med.* **14**, 140 (1990).
4. D. J. Lurie, I. Nicholson, M. A. Foster, and J. R. Mallard, *Phil. Trans. Roy. Soc. Lond.* **A333**, 453 (1990).
5. A. Iannone, A. Tomasi, V. Quaresima, and M. Ferrari, *Res. Chem. Intermed.* **19**, 715 (1993).
6. R. C. Brasch, *Radiology* **183**, 1 (1992).
7. H. J. Halpern, M. Peric, C. Yu, E. D. Barth, G. V. R. Chandramouli, M. W. Makinen, and G. M. Rosen, *Biophys. J.* **71**, 403 (1996).
8. D. A. Hall, D. C. Maus, G. J. Gerfen, S. J. Inati, L. R. Becerra, F. W. Dahlquist, and R. G. Griffin, *Science* **276** (5314), 930 (1997).
9. A. W. Overhauser, *Phys. Rev.* **92**, 411 (1953).
10. T. R. Carver and C. P. Slichter, *Phys. Rev.* **92**, 212 (1953).
11. I. Solomon, *Phys. Rev.* **99**, 559 (1955).
12. S. Un, T. Prisner, R. T. Weber, M. J. Seaman, K. W. Fishbein, A. E. McDermott, D. J. Singel, and R. G. Griffin, *Chem. Phys. Lett.* **189**, 54 (1992).
13. H. M. Swartz and J. F. Glockner, in "EPR Imaging and *in Vivo* EPR" (G. R. Eaton, S. S. Eaton, and K. Ohno, Eds.), CRC Press, Boca Raton, FL (1991).
14. I. Seimenis, M. A. Foster, D. J. Lurie, J. M. S. Hutchison, P. H. Whiting, and S. Payne, *Mag. Reson. Med.* **37**, 552 (1997).
15. I. Bertini, G. Martini, and C. Luchinat, in "Handbook of Electron Spin Resonance. Data Sources, Computer Technology, Relaxation, and ENDOR" (C. P. Poole and H. A. Farrach, Eds.), AIP Press, New York (1984).
16. S. J. McCallum, Ph.D. Thesis, University of Aberdeen, Aberdeen, UK (1997).
17. S. Andersson, G. J. Ehnholm, K. Golman, M. Jurjgensen, J. S. Petersson, F. Rise, O. Salo, and S. Vahasalo, *Radiology* **177**, 246 (1990).
18. S. Andersson, F. Radner, A. Rydbeck, R. Servin, and L. G. Wistrand, Nycomed Imaging AS, Oslo, Norway, U.S. Patent No. 5530140: Free Radicals (1996).
19. J. H. Ardenkjaer-Larsen, I. Laursen, I. Leunbach, G. Ehnholm, L. G. Wistrand, J. S. Petersson, and K. Golman, *J. Magn. Reson.* **133**, 1 (1998).
20. K. Golman, I. Leunbach, J. H. Ardenkjaer-Larsen, G. J. Ehnholm, L. G. Wistrand, J. S. Petersson, A. Jarvi, and S. Vahasalo, *Acta Radiologica* **39**, 10 (1998).

21. P. Kuppusamy, P. Wang, M. Chzhan, and J. L. Zweier, *Mag. Reson. Med.* **37**, 479 (1997).
22. H. Konijnenburg, J. Trommel, J. H. Ardenkjaer-Larsen, and A. F. Mehlkopf, "Proc., ISMRM, 5th Annual Meeting, Vancouver, Canada, 1997," p. 2129.
23. I. Nicholson, Ph.D. Thesis, University of Aberdeen, Aberdeen, UK (1991).
24. J. M. S. Hutchison, W. A. Edelstein, and G. J. Johnson, *J. Phys. E: Sci. Instrum.* **13**, 947 (1980).
25. J. S. Hyde and W. Froncisz, in "Advanced EPR: Applications in Biology and Biochemistry" (A. J. Hoff, Ed.), Elsevier, Amsterdam (1989).
26. C. P. Keijzers, E. J. Reijerse, and J. Schmidt, "Pulsed EPR: A New Field of Applications," North Holland, Amsterdam (1989).
27. E. L. Gintzon, "Microwave Measurements," McGraw-Hill, New York (1957).
28. M. K. Bowman, in "Modern Pulsed and Continuous-Wave Electron Spin Resonance" (L. Kevan and M. K. Bowman, Eds.), Wiley-Interscience, New York (1990).
29. G. A. Rinard, R. W. Quine, S. S. Eaton, G. R. Eaton, and W. Froncisz, *J. Magn. Reson. A* **108**, 71 (1994).
30. M. Alecci, J. A. Brivati, G. Placidi, L. Testa, D. J. Lurie, and A. Sotgiu, *J. Magn. Reson.* **132**, 162 (1998).
31. M. Alecci, Ph.D. Thesis, University of Aberdeen, Aberdeen, UK (1998).